OIKOS

Research

Stable nitrogen isotope analysis of amino acids as a new tool to clarify complex parasite–host interactions within food webs

Philip M. Riekenberg, Tijs Joling, Lonneke L. IJsseldijk, Andreas M. Waser, Marcel T. J. van der Meer and David W. Thieltges

P. Riekenberg (https://orcid.org/0000-0002-6275-5762) ✉ (phrieken@gmail.com), T. Joling (https://orcid.org/0000-0002-5705-3109) and M. van der Meer (https://orcid.org/0000-0001-6454-1752), Dept of Marine Microbiology and Biogeochemistry, NIOZ Royal Netherlands Inst. for Sea Research, Texel, the Netherlands. – TJ, A. M. Waser (https://orcid.org/0000-0002-9455-4447) and D. W. Thieltges (https://orcid.org/0000-0003-0602-0101), Dept of Coastal Systems, NIOZ Royal Netherlands Inst. for Sea Research, Texel, the Netherlands. – L. L. IJsseldijk (https://orcid.org/0000-0001-7288-9118), Division of Pathology, Dept of Biomolecular Health Sciences, Faculty of Veterinary Medicine, Utrecht Univ., Utrecht, the Netherlands. AMW also at: Alfred Wegener Inst., Helmholtz Centre for Polar and Marine Research, Wadden Sea Station Sylt, Sylt, Germany.

Oikos
130: 1650–1664, 2021
doi: 10.1111/oik.08450

Subject Editor: Jotaro Urabe
Editor-in-Chief: Dries Bonte
Accepted 7 June 2021

Traditional bulk isotopic analysis is a pivotal tool for mapping consumer–resource interactions in food webs but has largely failed to adequately describe parasite–host relationships. Thus, parasite–host interactions remain undescribed in food web frameworks despite these relationships increasing linkage density, connectance and ecosystem biomass. Compound-specific stable isotopes from amino acids provides a promising novel approach that may aid in mapping parasite–host relationships in food webs. Here we apply a combination of traditional bulk stable isotope analyses and compound-specific isotopic analysis of nitrogen in amino acids to examine resource use and trophic interactions of five parasites from three hosts from a marine coastal food web (Wadden Sea, European Atlantic). By comparing isotopic compositions of bulk and amino acid nitrogen, we aimed to characterize isotopic fractionation occurring between parasites and their hosts and to clarify parasite trophic positions. Our results indicate that parasitic trophic interactions were more accurately identified using compound-specific stable isotope analysis due to removal of underlying source isotopic variation for both parasites and hosts. The compound-specific method provided clearer trophic discrimination factors in comparison to bulk isotope methods. Amino acid compound specific isotope analysis has widely been applied to examine trophic position within food webs, but our analyses suggest that the method is particularly useful for clarifying the feeding strategies for parasitic species. Baseline isotopic information provided by source amino acids allows clear identification of the fractionation from parasite metabolism by integrating underlying isotopic variations from the host tissues. However, like for bulk isotope analysis, the application of a universal trophic discrimination factor to parasite–host relationships remains inappropriate for compound-specific stable isotope analysis. Despite this limitation, compound-specific stable isotope analysis is and will continue to be a valuable tool to increase our understanding of parasitic interactions in marine food webs.

Keywords: parasite, trophic level, trophic position, Wadden Sea

Introduction

Bulk tissue stable isotope analysis (hereafter $\delta^{13}C_{bulk}$ or $\delta^{15}N_{bulk}$ and bulk-SIA) is routinely applied to identify resource utilization and trophic interactions within food webs (Minagawa and Wada 1984, Fry 2006). Trophic positions (TP) are identified through application of one (Post 2002, McCutchan et al. 2003) or several (Hussey et al. 2014) trophic discrimination factors (TDFs) for consumers describing the difference in isotopic composition between the consumer and their diet (Δ) for carbon or nitrogen. However, application of system-wide or group-specific TDFs do not reliably account for parasite–host relationships, which have TDFs varying from −6.7‰ to 9.0‰ (Thieltges et al. 2019) for $\delta^{15}N_{bulk}$. These values fall well outside of the ranges typically observed for $\delta^{15}N_{bulk}$ TDFs for consumers (McCutchan et al. 2003, Mill et al. 2007, Caut et al. 2009) and span across parasitic species (Pinnegar et al. 2001, Dubois et al. 2009), feeding styles and host tissue specificity, indicating that TDFs for parasites may be specific to each relationship (Lafferty et al. 2008, Thieltges et al. 2019).

Parasitism describes a trophic interaction between two species where the parasite lives in or on the host and obtains part of, or all of, its nutritional requirements through feeding on its host, with a negative effect for the host (Lafferty and Kuris 2002). Parasitism is a widespread lifestyle, with ~40% of all organisms having at least one parasitic life-stage. Accounting for parasitic relationships, ~75% of food web interactions involve a parasite (Dobson et al. 2008) causing increases in linkage density (Lafferty et al. 2008, Sánchez Barranco et al. 2020), food chain length (Amundsen et al. 2009) and connectance (Dunne et al. 2013). Contributions of parasite biomass to an ecosystem can be substantial and even exceed that of top predators (Kuris et al. 2008, Preston et al. 2013). Despite widespread occurrence of parasites throughout ecosystems, these relationships have been neglected during construction of food webs since they are often incompletely understood and/or described (Marcogliese and Cone 1997, Lafferty et al. 2008). Incomplete characterizations of parasite–host relationships are due to the cryptic nature of interactions resulting from the difficulty of reliable sampling during the complex life-cycles of many parasite (Goater et al. 2014).

Several mechanisms potentially contribute to variability in TDFs for parasitic relationships: 1) mismatch between measured tissue type and tissue use by parasite, 2) incorporation of multiple materials depending on parasite feeding style and 3) differing abilities in directly acquiring, anabolizing or metabolizing amino acids between parasites (Riekenberg et al. 2021a). Many studies examining parasite–host isotopic differences used host muscle tissue despite local parasite attachment to or inhabiting another organ or tissue. Tissue mismatch can cause erroneous $\Delta^{15}N$ values for parasites feeding on non-muscle host tissue (Pinnegar et al. 2001, Kamiya et al. 2019). Parasite feeding styles vary, from external blood suckers to mixed diet intestinal feeders (Goater et al. 2014) resulting in variations in parasite dietary compositions ranging from complete reliance on host tissue to predominately host gut contents (Deudero et al. 2002, Goedknegt et al. 2018a). Metabolic abilities of parasites such as helminths are often less complete than those found in vertebrates (Tyagi et al. 2015) leading to variability in biosynthesis capabilities and metabolism of compounds between species, even within the same phylum. Metabolic limitations arise when parasites can directly utilize amino acids or lipids from their hosts without requiring additional metabolism that results in variable $\Delta^{13}C$ or $\Delta^{15}N$ values (Deudero et al. 2002, Power and Klein 2004, O'Grady and Dearing 2006), such as transamination or lipid synthesis pathways that occur along different metabolic pathways other than normally observed in vertebrate trophic relationships (O'Connell 2017). Impacts on $\Delta^{15}N$ values resulting from unique metabolism and feeding styles can confound determination of whether a parasite is feeding on its host or supplementing with other resources (e.g. gut content) based on bulk-SIA methods alone.

Compound-specific stable isotope analysis (CSIA) of nitrogen from amino acids (AA), hereafter $\delta^{15}N_{AA}$ and AA-CSIA, provides a potential solution by simultaneously resolving baseline changes from trophic effects between parasites and hosts (Chikaraishi et al. 2007, Sabadel et al. 2016). This information comes from amino acids occurring in three types: 1) source, that undergo minimal change during metabolism and strongly retain a signal of underlying nitrogen being utilized (e.g. host or dietary N); 2) trophic, with stepwise increases as they are metabolized via transamination; and 3) metabolic, which change due to physiological processes in the animal or whether particular processing pathways are present (Popp et al. 2007, Chikaraishi et al. 2009, McMahon and McCarthy 2016). Using AAs, TPs can be estimated by using the $\delta^{15}N$ value difference between a trophic and a source AA combined with system-wide values for TDFs and the $\Delta^{15}N$ between trophic and source AAs in the underlying primary producers (Chikaraishi et al. 2009, Whiteman et al. 2019). In parasite–host relationships, $\delta^{15}N_{AA}$ allows for isolation of the metabolism and feeding style effects because it resolves underlying shifts in baseline $\delta^{15}N$ value for host or parasite to further clarify the trophic interaction. Although very promising, $\delta^{15}N_{AA}$ in parasite studies has barely been utilised. A single study confirmed a large bulk $\Delta^{15}N$ difference between a scarab beetle larvae and a mite (7.5‰, 2.2 TP) matched the difference found with $\delta^{15}N_{AA}$ (1.8 TP) indicating a mutualistic relationship rather than parasitism between the pair (Sabadel et al. 2016, 2019). To the authors knowledge there have been no studies that use $\delta^{15}N_{AA}$ for parasite–host relationships with a $\Delta^{15}N_{Bulk}$ value below the typically applied TDF value of 3.4‰.

In this study, we apply and compare results from both bulk-SIA and AA-CSIA analyses applied to five parasites from three common host species from a marine coastal food web (Dutch Wadden Sea). The five parasite–host pairings analysed in this study are 1) the copepod *Mytilicola orientalis*–Pacific oyster *Magallana gigas*, 2) the parasitic barnacle *Sacculina carcini*–shore crab *Carcinus maenas*, 3) lung *Pseudaliida*, 4) stomach *Aniskis simplex* and 5) ear nematodes *Stenurus minor*–harbour

porpoise *Phocoena phocoena*. We are the first to apply $\delta^{15}N_{AA}$ to examine parasite–host relationships in a range of marine animals that span the breadth of trophic positions present in coastal marine food webs with oysters *M. gigas* as primary consumers, green shore crabs *C. maenas* as secondary consumers and harbour porpoise *P. phocoena* as an apex predator. Here we: 1) identify whether AA-CSIA improves characterization of parasite–host relationships compared to bulk-SIA, 2) identify the AA fractionations driving these differences and 3) determine whether use of locally-associated host tissue improves indications of trophic relationships.

Material and methods

Parasite–host relationships of the studied species

Magallana gigas is a filter-feeding bivalve (primary consumer) that is considered an invasive species in the Wadden Sea (Troost 2010, Jung et al. 2019) and is host to several macroparasites including the copepod *Mytilicola orientalis* (Stock 1993, Thieltges et al. 2013). *Mytilicola orientalis* has a direct life cycle with a short non-feeding free-living stage, after which it permanently lives in the intestines of its host, but its feeding strategy remains incompletely characterized (Goedknegt et al. 2018b).

Carcinus maenas, is a crab native to the Wadden Sea and is a secondary consumer that feeds as a generalist (Mente et al. 2010). *Carcinus maenas* is host to a diverse set of parasites including nematodes, trematodes, cestodes and isopods (Zetlmeisl et al. 2011), but we focused on the parasitic rhizocephalan barnacle *Sacculina carcini*. Larval *S. carcini* infect their crustacean host by invading the carapace and developing during maturation an extensive root system specialised to directly absorb nutrients from a variety of tissues/internal organs (e.g. muscle, hepatopancreas and the nervous system; Lützen 1984). *Sacculina carcini* has no mouth, gut, respiratory organs, excretory organs or an alimentary canal during its parasitic life cycle stage (Bresciani and Høeg 2001). The effects of an infection by *S. carcini* on *C. maenas* include: parasitic castration, behavioural feminization of males, tissue changes, growth limitation or even a complete stop of the moult cycle (Powell and Rowley 2008, Kristensen et al. 2012, Waser et al. 2016). The reproductive organ of *S. carcini*, the so-called externa, develops outside of its host and is the only body part visible to the naked eye.

Phocoena phocoena, are small cetaceans inhabiting coastal waters and are generalist feeders on small fish like herring, sprat and anchovy (Jansen et al. 2013, Leopold 2015) and they are host to a diverse range of parasites including cestodes, nematodes, trematodes, crustaceans and acanthocephala (Brosens et al. 1996, Herreras et al. 1997). In this study we examined lung, ear and stomach nematodes (Goater et al. 2014) found during necropsies of *P. phocoena* stranded on Dutch beaches. There are multiple species of nematodes parasitizing the lungs of *P. phocoena* (Lehnert et al. 2005) and in this study individuals from the *Pseudaliidae* family, likely *Pseudalius inflexus* or *Torynurus convolutes*, were analysed. Both nematodes have heteroxenous life cycles (Lehnert et al. 2010) and are very common parasites that can occur without causing health problems for their host *P. phocoena* (Lehnert et al. 2005, ten Doeschate et al. 2017), although severe infestations can limit the lung capacity, induce infections and reduce fitness. Little is known about the life cycle of the ear nematode, *Stenurus minor*, but it is likely that invertebrates and vertebrates serve as intermediate or paratenic hosts for this parasite (Faulkner et al. 1998). Although rare, there have been reports of noise-induced hearing damage due to *S. minor* infestations in the inner ear of a harbour porpoise (Morell et al. 2017). The stomach nematode, *Anisakis simplex*, has a complex life cycle which includes a free-living stage, 1 or 2 intermediate crustacean hosts and 1 or 2 paratenic fish hosts. Marine mammals are the final host of *A. simplex* (Nagasawa 1990) where the parasite occurs in the stomach and has been associated to a lowered nutritional condition of its host (ten Doeschate et al. 2017). It is however unclear whether *A. simplex* lowers the nutritional condition, or that harbour porpoises with a low nutritional condition are more susceptible to infections. Larval *A. simplex* that enter the stomach are thought to feed on the food bolus, but often penetrate the stomach lining and appear to feed upon host tissue (Gibson et al. 1998) and are known to cause anisakiasis due to attachment and extrusion of proteolytic enzymes into the gastric mucosa (Pravettoni et al. 2012).

Sample collection

Magallan gigas was collected by hand during low tide in April 2019 from the Mokbaai, Texel, the Netherlands (53°00′22.4″N, 4°46′03.9″E). Oysters were kept alive in a tank with aerated sea water at a controlled temperature (15°C) prior to dissection. Of the 111 dissected oysters, 27 were infected with at least one *M. orientalis* individual (24% prevalence). *Mtilicola orientalis* individuals were removed from the oyster under a dissecting microscope and host tissue was sampled from the adductor muscle of the infected oysters. Parasite and host tissue samples were rinsed with deionized water after sampling, further confirmed to be free of excess tissues from host, and frozen (−20°C) immediately following dissection.

A beam trawl was used to collect *S. carcini* infected crabs in the Western Wadden Sea (52°59′50.5″N, 4°51′02.4″E) in May of 2019. Infected crabs (identified by the presence of an externa) were separated from bycatch directly after each trawl on deck of the ship and uninfected *C. maenas* were returned overboard directly. A total of 27 infected *C. maenas* individuals were sampled with an estimated infection prevalence of less than 1%. Infected hosts were maintained in aerated seawater at a controlled temperature (15°C) prior to dissection. The *S. carcini* externa, *C. maenas* hepatopancreas and clawmuscle tissues were dissected under a magnifying desk lamp. The *S. carcini* and host tissues were rinsed with deionized water after sampling, further confirmed to be free of excess tissues from host, and frozen (−20°C) immediately following dissection.

Samples were collected from stranded harbour porpoises which were found dead on Dutch beaches during March 2019. Shortly after stranding, the *P. phocoena* were necropsied as part of a long-term monitoring programme at the Faculty of Veterinary Medicine, Utrecht University, the Netherlands. Dorsal muscle (*M. Longissimus dorsi*) tissue was sampled from eight harbour porpoises and parasitic nematodes, if present, were sampled (lung, n = 8; ear, n = 7; stomach wall, n = 5) as well as the locally associated organ tissue of the host. All samples were stored frozen (−20°C), prior to transport to NIOZ. Here, tissues were sub-sampled, rinsed with deionized water, and any remaining foreign remnant tissues from dissected tissues were removed.

The animals described in this study were free-living harbour porpoises which died of natural causes and not for the purpose of this, or other, studies. No consent from an Animal Use Committee is required, as the animals described in this study were not used for scientific or commercial testing. Consequently, animal ethics committee approval was not applicable to this work.

Bulk and amino acids stable isotope analysis

All sample tissues (< 1 g wet weight) were frozen (−20°C) immediately after dissection and lyophilized within two weeks of sampling. Lyophilized tissues were ground using a mortar and pestle. Crab hepatopancreas and *S. carcini* samples were lipid extracted prior to analysis. Tissue samples were then loaded into tin capsules for bulk-SIA analysis using an isotope ratio mass spectrometer with an element analyzer. The reference materials acetanilide, urea and casein, were standards for stable isotope measurements for $\delta^{13}C$ and $\delta^{15}N$ expressed as per mil (‰) differences from the $\delta^{13}C$ value of Vienna Peedee-Belemnite Limestone (VPDB) and the $\delta^{15}N$ value of atmospheric N_2. Sample precision was ± 0.1‰ and ± 0.2‰ for $\delta^{13}C$ and $\delta^{15}N$, respectively, for bulk material supporting this study.

For CSIA-AA analysis, dried and homogenized tissue (2–5 mg) was lipid extracted, acid hydrolyzed, derivatized to pivaloyl–isopropyl esters and analysed for $\delta^{15}N$ of AAs via gas chromatography–combustion isotope mass spectrometry following the method presented in Riekenberg et al. (2021b). $\delta^{15}N$ values for 14 AAs are reported: alanine (Ala), aspartic acid (Asp), glutamic acid (Glu), glycine (Gly), leucine (Leu), lysine (Lys), isoleucine (Ile), methionine (Met), phenylalanine (Phe), proline (Pro), serine (Ser), threonine (Thr), tyrosine (Tyr) and valine (Val). Precision of amino acid $\delta^{15}N$ values were < 0.5‰ in standards run 10× per sequence for 14 AAs throughout the analytical runs supporting this study and sample duplicates had an average precision of 0.24‰. Normalization using two standard reference mixtures along with a reference spike of norleucine (Nle) added to all samples and standards which served as an internal reference calibration following the method from Yarnes and Herszage (2017).

Parasite–host differences and trophic position

Parasite–host differences for $\Delta^{15}N_{Bulk}$ and $\Delta^{13}C_{Bulk}$ were calculated for each parasite–host pair separately by subtracting the isotope ratio of host tissue from the isotope ratio of the associated parasite. For parasites of crabs and harbour porpoises this was reported for both muscle and locally-associated host tissues. Trophic position estimates were calculated using $\delta^{15}N$ values from bulk material:

$$TP_{Bulk} = 1 + \frac{\delta^{15}N_{Bulk} - \delta_{Bulk}}{TDF_{Bulk}} \quad (1)$$

where β_{Bulk} is the $\delta^{15}N$ value for primary producers in the ecosystem (9.44‰; Goedknegt et al. 2018a), TDF_{Bulk} is the difference between consumer and their diet (3.4‰; DeNiro and Epstein 1978, Minagawa and Wada 1984).

Trophic position estimates using CSIA-AA were calculated using two approaches:

1) $\delta^{15}N$ values from only one trophic AA and one source AA, Glu and Phe, respectively:

$$TP_{Glu\text{-}Phe} = 1 + \frac{\delta^{15}N_{Glu} - \delta^{15}N_{Phe} - \beta}{TDF_{Glu\text{-}Phe}} \quad (2)$$

Table 1. $\delta^{15}N_{Bulk}$ and $\delta^{13}C_{Bulk}$ data for each parasite (bold text) and host tissue pairing.

Host	Host tissue or parasite	No. of samples	$\delta^{13}C$ (‰)		$\delta^{15}N$ (‰)	
			Mean	SD	Mean	SD
M. gigas	Muscle	22	−17.8	0.3	11.7	0.4
	M. orientalis	22	−18.5	0.3	11.7	0.4
C. maenas	Muscle	26	−16.7	0.8	14.2	0.6
	Hepatopancreas	27	−17.6	0.6	13.5	0.9
	S. carcini	27	−17.7	0.6	14.1	0.5
P. phocoena	Muscle	8	−17.9	0.5	15.8	1.2
	Lung	8	−17.8	0.7	17.7	1.8
	Ear canal	7	−19.3	1.5	17.4	1.3
	Stomach	6	−17.2	0.4	16.6	1.3
	Lung nematode	8	−18	0.8	17.7	1.7
	Ear nematode	7	−16.8	0.5	21.8	1
	Stomach nematode	6	−17	1.6	15.1	2.1

where $TDF_{Glu\text{-}Phe}$ represents the expected stepwise increase between consumer and diet for $\delta^{15}N$ value of Glu with each trophic step and β represents the difference between Glu and Phe within the primary producer at the base of the food web (Chikaraishi et al. 2009). A $TDF_{Glu\text{-}Phe}$ of 6.6‰ and a $\beta_{Glu\text{-}Phe}$ of 2.9‰ were applied from the meta-analysis presented in Nielsen et al. (2015).

2) An equation using four trophic and one source AA (TP_{5AA}) as described in Nielsen et al. (2015):

$$TP_{5AA} = 1 + \frac{\left(\begin{array}{l}\delta^{15}N_{Glu} + \left(\delta^{15}N_{Leu} + 2.93\right) \\ + \left(\delta^{15}N_{Ile} - 2.63\right) + \left(\delta^{15}N_{Val} + 3.35\right)\end{array}\right) / 4 - \delta^{15}N_{Phe} - \beta_{x/y}}{\Delta_x - \Delta_y} \quad (3)$$

where the TP_{5AA} method incorporates more AAs than the $TP_{Glu\text{-}Phe}$ method and is less affected by outlying measurements from individual AAs. Incorporating more source and trophic AAs reduces TP variation and gives a more precise estimation of TP. The $\delta^{15}N_{AA}$ values of Leu, Ile and Val are normalized to the $\delta^{15}N_{Glu}$ value using the values 2.93, 2.63 and 3.35‰, respectively (Nielsen et al. 2015) which allows for the calculation of a single mean $\delta^{15}N_{AA}$ value using multiple trophic AAs using calculated $\beta_{x/y} = 2.9‰$ and $\Delta_x - \Delta_y = 5.9‰$.

AA imbalance represents the AA concentration in host tissue compared to the parasite's tissue composition. AA imbalance was calculated by subtracting the concentration of individual AAs (mg g^{-1}) in the locally-associated host tissue from the corresponding parasite tissue concentration (McMahon et al. 2015).

Statistical analyses

Pairwise t-test and Wilcoxon tests were used to examine parasite–host differences in bulk $\delta^{13}C$ and $\delta^{15}N$ values, $\delta^{15}N$ values for individual amino acids, TP differences, as well as differences between bulk TP and $TP5_{AA}$ as appropriate following Shapiro–Wilks tests for normality. A Pearson correlation was used to compare C:N ratios, AA imbalance and $\Delta^{15}N_{Bulk}$ values for the lung and ear nematode-*P. phocoena* pairings. Principal component analyses were applied to the individual amino acid $\delta^{15}N$ differences between parasite and locally-associated host tissue pairs. A complete listing of the results from pairwise t-tests can be found in the Supporting information.

Results

Bulk isotope comparisons

Between host comparisons for bulk isotope data can be found in the Supporting information. Pairwise t-tests and Wilcoxon tests (for non-normally distributed measurements) describe $\delta^{13}C$ and $\delta^{15}N$ comparisons between parasites and host tissues as appropriate following Shapiro–Wilk tests for normality. *Mytilicola orientalis* (−18.5 ± 0.3‰; Table 1, Fig. 1) and *Sacculina carcini* (−17.7 ± 0.6‰) had lower $\delta^{13}C_{Bulk}$ values than their host muscle tissue, oyster adductor (−17.8 ± 0.3‰; $t_{21} = -8.60$, $p < 0.001$) and crab claw-muscle (−16.7 ± 0.8‰; $t_{25} = -5.26$, $p < 0.001$), respectively. However, the $\delta^{13}C$ value of *S. carcini* did not differ from locally-associated host hepatopancreas (−17.6 ± 0.6‰; $t_{25} = -1.82$, $p = 0.08$). The $\delta^{13}C$ value of lung (−18.0 ± 0.8‰) and stomach nematodes (−17.0 ± 1.6‰) were similar to both harbour porpoise muscle tissue (−17.9 ± 0.4‰; $t_7 = -0.79$, $p = 0.46$; $t_5 = 1.69$, $p = 0.15$) and locally-associated host tissues (lung: −17.8 ± 0.7‰; $t_7 = -1.07$, $p = 0.32$ and stomach: −17.2 ± 0.4‰; $t_5 = 0.35$, $p = 0.74$). The ear nematode (−16.8 ± 0.5‰) had a higher $\delta^{13}C_{Bulk}$ value compared to harbour porpoise muscle ($p < 0.001$) and locally-associated ear tissue (−19.3 ± 1.5‰; $t_6 = 5.28$, $p < 0.01$).

Mytilicola orientalis (11.7 ± 0.4‰) had no significant $^{15}N_{Bulk}$ enrichment compared to its oyster host (11.7 ± 0.4‰; $t_{21} = 0.1$, $p = 0.91$). The $\delta^{15}N_{Bulk}$ value of *S. carcini* (14.1 ± 0.5‰) did not differ from the claw tissue of its host (14.2 ± 0.6‰; $t_{25} = -1.06$, $p = 0.30$) but was higher compared to locally-associated hepatopancreas (13.5 ± 0.9‰; $W = 58$, $p < 0.01$). The $\delta^{15}N_{Bulk}$ value of lung nematode (17.7 ± 1.7‰) was higher than harbour porpoise muscle tissue (15.8 ± 1.1‰; $t_7 = 7.30$, $p < 0.001$), but comparable to locally-associated lung tissue (17.7 ± 1.8‰; $t_7 = -0.09$, $p = 0.93$). The $\delta^{15}N_{Bulk}$ value of the stomach nematode (15.1 ± 2.1‰) was similar to harbour porpoise muscle (15.8 ± 1.1‰; $W = 6$, $p = 0.43$) and stomach tissue (16.6 ± 1.3‰; $W = 18$, $p = 0.16$). The ear nematodes had the highest $\delta^{15}N_{Bulk}$ value (21.8 ± 1.0‰), higher than both harbour porpoise muscle ($p < 0.001$) and locally-associated ear tissue (17.4 ± 1.3‰; $t_6 = 26.55$, $p < 0.001$).

Amino acid isotope comparisons

$\delta^{15}N_{AA}$ values were similar for the different tissues from the same host, with Val, Ala, Glu, Asp, Leu, Ile and Pro having higher values representative of trophic AAs, Tyr, Phe, Met, Lys

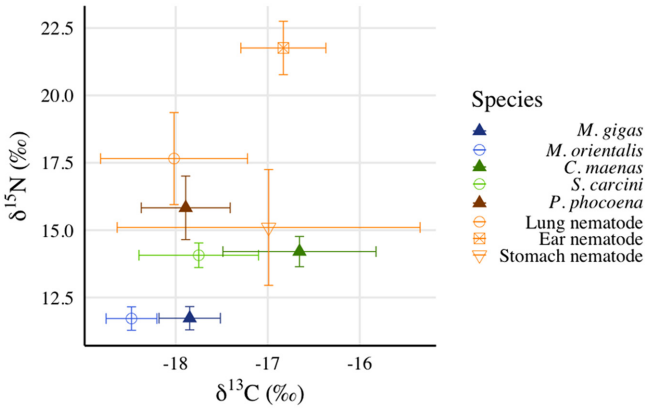

Figure 1. $\delta^{15}N_{Bulk}$ and $\delta^{13}C_{Bulk}$ data of parasites (open symbols) and hosts (full symbols). Mean $\delta^{15}N_{Bulk}$ and $\delta^{13}C_{Bulk}$ values for: *M. gigas*–*M. orientalis*, *C. maenas*–*S. carcini* and *P. phocoena*–parasitic nematodes (mean ± SD). For n see Table 1.

and Gly, Ser, Thr having lower values associated with source and metabolic AA groupings, respectively. Pairwise t-tests (Supporting information) indicated significant differences between parasite and host trophic AAs in *M. orientalis*-oyster (Fig. 2A), *S.carcini*-crab (Fig. 2B), ear nematode–harbour porpoise and the lung nematode–harbour porpoise relationships, but not for the stomach nematode–harbour porpoise relationship (Fig. 3A–C). All parasite–host pairings were significantly different for at least one of the source AAs, but differences were variable in magnitude and direction. The largest difference observed for source AAs was for Tyr in the ear nematode–harbour porpoise pairing for muscle (18.3‰; $t_5 = 14.29$, $p < 0.01$) and ear (18.8‰; $t_5 = 24.25$, $p < 0.01$) tissues. All parasite–host pairings except for *S. carcini*-crab

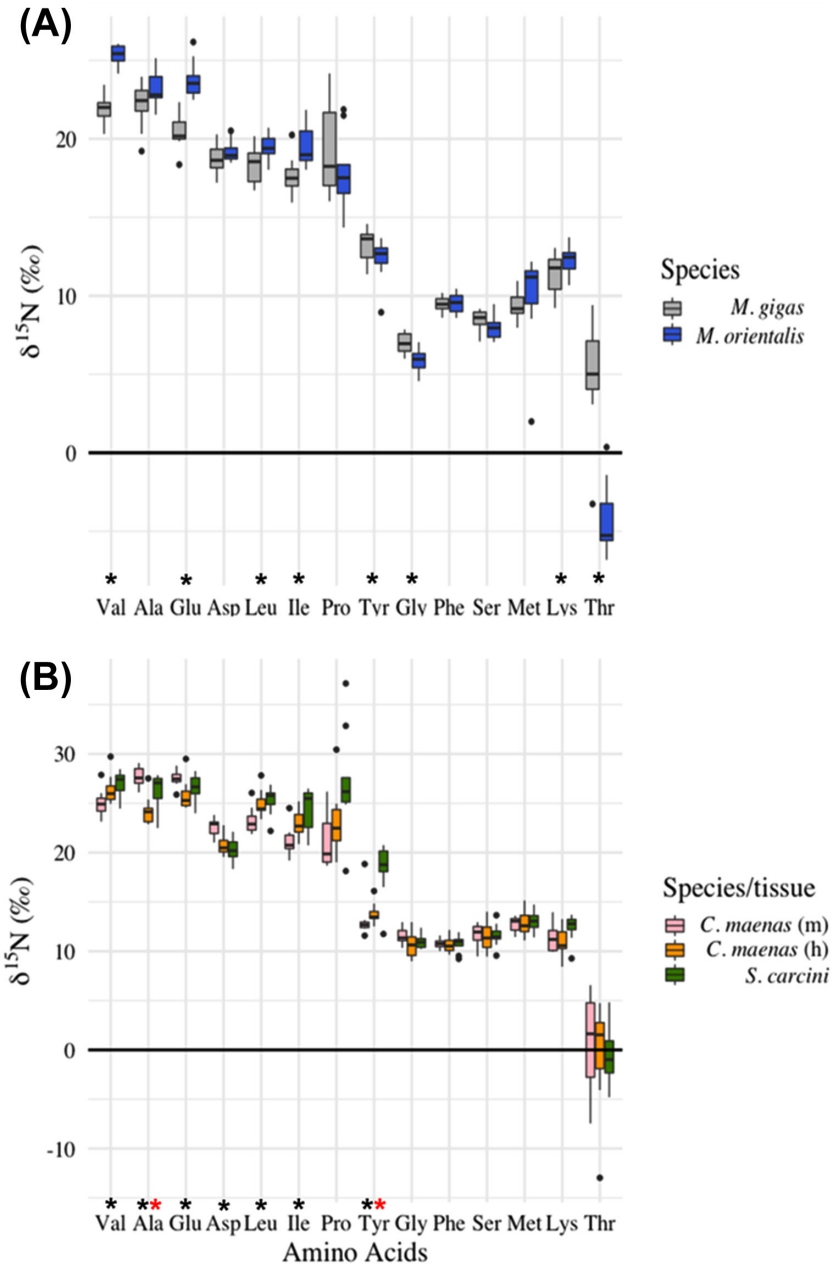

Figure 2. $\delta^{15}N$ values for amino acids in (A) *M. orientalis–M. gigas* and (B) *S. carcini–C. maenas* parasite–host pairings. Median $\delta^{15}N_{AA}$ values (solid line) are presented for 14 AAs for 12 pairings for *M. orientalis* and 11 pairings for *S. carcini*. Significant pair-wise differences (*$p < 0.05$) are indicated between parasite and host tissue using t-tests or Wilcoxon tests depending on normal distribution as indicated by Shapiro–Wilk tests for normality for each pairing. Black asterisks indicate parasite–host muscle (m) tissue differences while red asterisks indicate parasite–host local tissue differences e.g. hepatopancreas (h). Boxes and error bars represent 25th and 10th percentiles, respectively, and dots represent outliers. AA order was determined by relative fractionation difference and do not reflect the groupings defined by the PCA analysis.

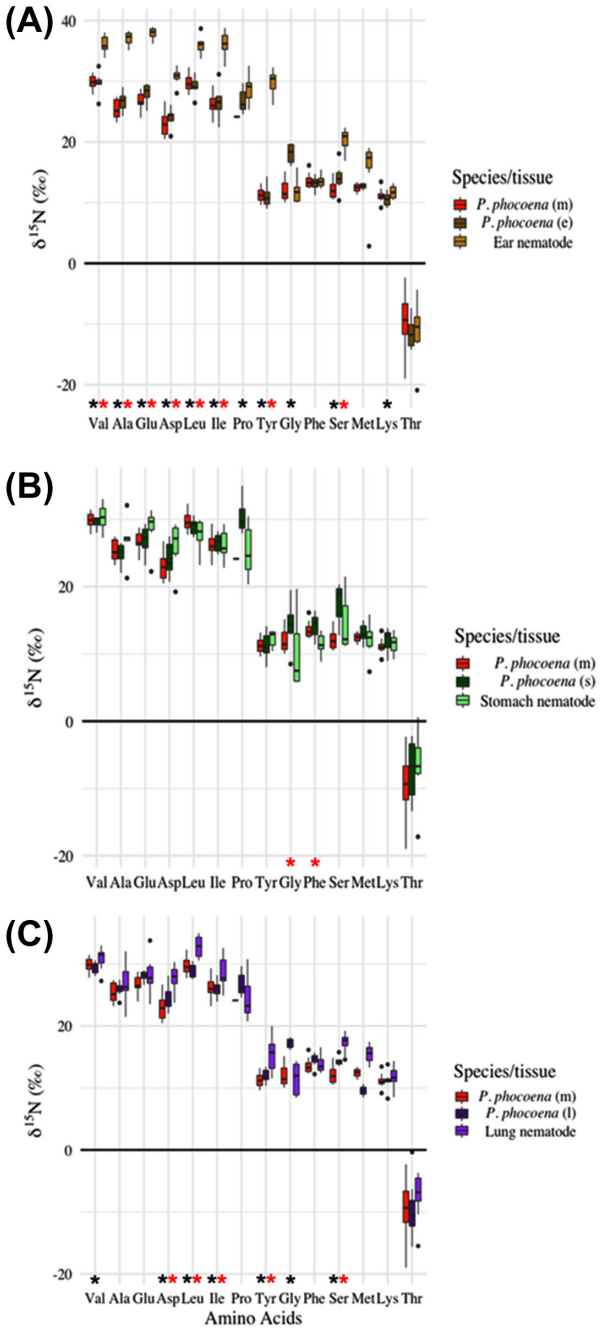

Figure 3. $\delta^{15}N$ values for amino acids in (A) ear nematodes, (B) stomach nematodes and (C) lung nematodes from *P. phocoena* parasite–host pairings. Median $\delta^{15}N_{AA}$ values (solid line) are presented for 14 AAs for seven pairings for ear, six pairings for stomach and eight pairings for lung nematodes. Significant pair-wise differences (*$p < 0.05$) are indicated between parasite and host tissues using t-tests. Black asterisks indicate parasite–host muscle (m) tissue differences while red asterisks indicate parasite–host local tissue differences e.g. ear (e), stomach (s) or lung (l). Boxes and error bars represent 25th and 10th percentiles, respectively, and dots represent outliers. AA order was determined by relative fractionation difference and do not reflect the groupings defined by the PCA analysis.

had significant differences in metabolic AAs that varied in magnitude and direction. Gly differences between lung nematode and locally-associated lung tissue from harbour porpoise were large and negative (−5.7‰; $t_7 = -6.68$, $p < 0.01$) despite no difference occurring between parasite and host muscle tissue ($p = 0.7$).

Principal component analyses for $\delta^{15}N$ differences between parasite-locally-associated host tissue pairs indicate that the first principal component (PC1) explained 47–69% and the second principal component (PC2) explained 12–20% of the total $\delta^{15}N_{AA}$ variance (Fig. 4). The parasites *M. orientalis*, lung and ear nematodes were clearly separated from their respective hosts with non-overlapping 95% confidence intervals in multivariate space (Fig. 4A, C, D), while *S. carcini* and stomach nematodes were not separated from their host (Fig. 4B, E). The AAs in the principal component analysis largely grouped together according to the trophic, metabolic and source AA groupings that reflect fractionations associated with their metabolism. The ear and lung nematodes had positive loadings of similar magnitude for trophic AAs (Fig. 4C–D), but trophic AAs also drove contrasting negative loadings for PC1 for *M. orientalis* (Fig. 4A). Trophic AA loadings for PC2 were near zero in ear nematodes, small for *M. orientalis* and significant (both positive and negative) for lung nematodes (Fig. 2A, C, D). Loadings for Glu and Ala in lung nematodes were considerably different from the other trophic AAs and group with Lys, a source AA that did not differ in the lung nematode–lung tissue pairing (Fig. 4). Most loadings for source AAs were smaller across PC1, but values for PC2 remained larger in comparison to loadings observed for trophic AAs in *M. orientalis*, ear and lung nematodes (Fig. 2A, C, D). Source AAs were important loadings for PC2 in *M. orientalis*, ear and lung nematodes (Fig. 2A, C, D) with ear nematode being negative versus the other two positive relationships. Thr contributed to separation across PC1 for *M. orientalis* but did not contribute considerably to separations observed for other pairings.

Comparing trophic position estimates between methods

TP_{Bulk} (Fig. 5A), $TP_{Glu\text{-}Phe}$ (Fig. 5B) and TP_{5AA} (Fig. 5C) provided different trophic position estimates for parasites versus their hosts (ΔTP) between the methods (Fig. 5, 6 and Supporting information). Pairwise t-tests showed no difference in TP_{Bulk} for the *M. orientalis*-oyster pairing, but that $TP_{Glu\text{-}Phe}$ and TP_{5AA} were significantly different ($\Delta TP = 0.4$). The *S. carcini*-crab hepatopancreas pairing had similar TPs across methods, but when compared against host (crab) muscle tissue $TP_{Glu\text{-}Phe}$ decreased and TP_{5AA} increased. Lung parasite TP was higher than harbour porpoise muscle tissue for TP_{Bulk} and ΔTP_{5AA} but similar using $TP_{Glu\text{-}Phe}$. When the lung nematode was compared against locally-associated lung tissue, TP_{5AA} increased, but no difference was found for ΔTP_{Bulk} or $TP_{Glu\text{-}Phe}$. Ear nematodes had a higher TP compared to harbour porpoise muscle tissue and locally-associated ear tissue. Stomach

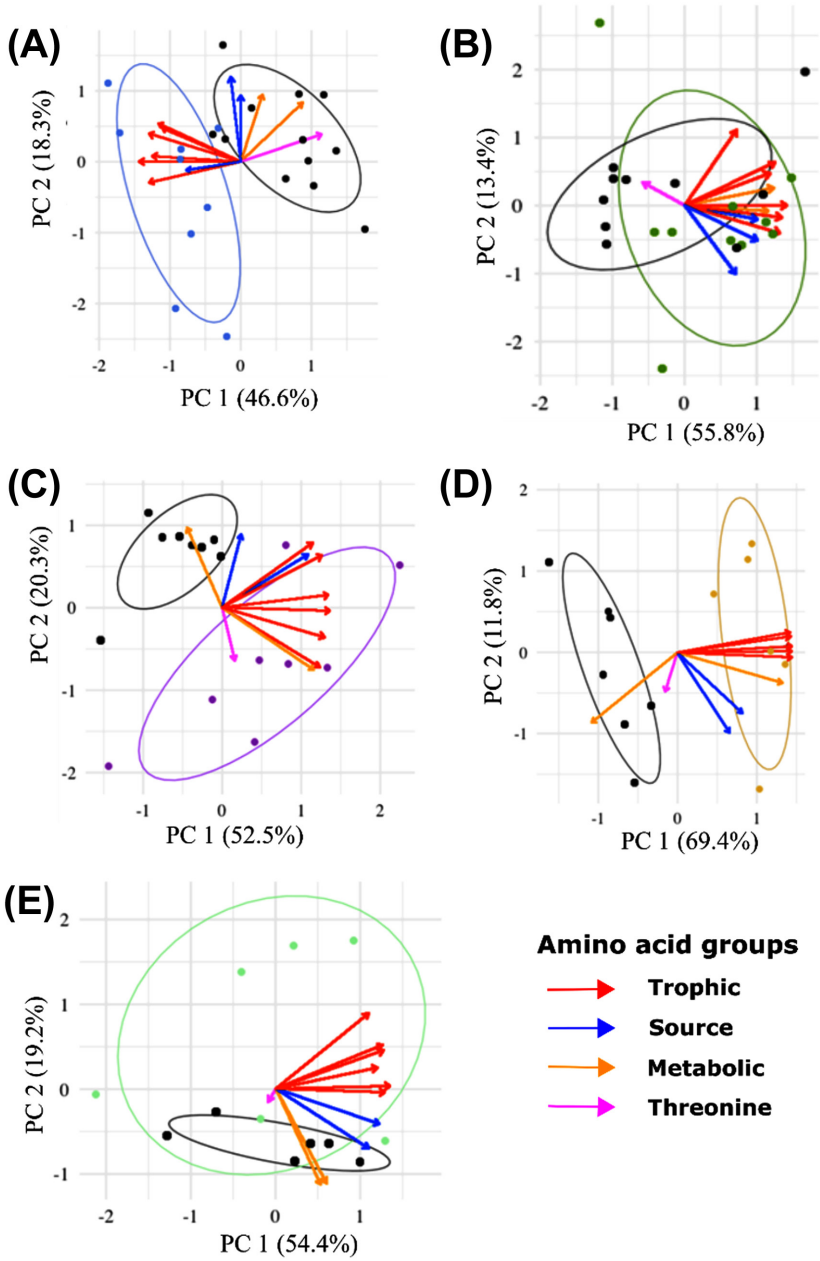

Figure 4. PCA biplots of parasite–host locally-associated tissue $\delta^{15}N_{AA}$ values for (A) *M. orientalis–M. gigas* (blue; n = 9)–(black; n = 12), (B) *S. carcini–C. maenas* hepatopancreas tissue (green; n = 10)–(black; n = 11), (C) lung nematode–*P. phocoena* lung tissue (violet; n = 8)–(black; n = 8), (D) ear nematode–*P. phocoena* ear tissue (ochre; n = 6)–(black; n = 7), (E) stomach nematode–*P. phocoena* stomach tissue (light green; n = 6)–(black; n = 6). The eigenvalues among $\delta^{15}N_{AA}$ values of the principal component is shown in brackets as % of variance explained. AAs are shown as eigenvectors in the plots, common fractionation behaviors are indicated by colour: red = trophic (Ala, Asp, Glu, Ile, Leu, Tyr, Val), blue = source (Phe, Lys, Met), orange = metabolic (Gly, Ser) and pink = Thr. The ellipses indicate the 95% CI for PC values of the organisms.

nematodes TP_{5AA} was higher than the harbour porpoise muscle tissue, but comparable for both ΔTP_{Bulk} and $TP_{Glu\text{-}Phe}$. However, stomach nematodes TP was higher than locally-associated stomach tissue for both $TP_{Glu\text{-}Phe}$ and TP_{5AA}, but comparable to TP_{Bulk}. Supporting information for all TP pairwise t-tests for different host tissue types and Supporting information for all pairwise t-tests between TP_{Bulk} and TP_{5AA}.

Discussion

This study identified considerable differences between $\Delta^{15}N$ values determined for parasite–host pairings using bulk-SIA (Fig. 1) and AA-CSIA (Fig. 2–4) causing different TP estimates for parasites between techniques. Changes in amino acid $\delta^{15}N$ values between parasite–host pairings confirmed expected groupings of source, trophic and metabolic amino

acids based on known metabolic pathways for AAs in consumers (Fig. 4). However, direct uptake and utilization of AAs appears to extensively occur in the parasite (*Sacculina carcini*) resulting in minimal fractionation and comparable TPs between the parasite and locally-associated host tissue (Fig. 4B, 6B). Differences in TP between parasite–host pairings among parasite species (Fig. 5) supports using species-specific fractionation factors when characterizing parasite relationships in food webs as well as targeted sampling of locally-associated host tissue that parasites are using. However, AA-CSIA improved the characterization of TDFs and metabolic pathways utilized for each parasitic interaction regardless of the tissue type used by providing a reliable indication of underlying $\delta^{15}N$ values from the resources (e.g. tissue or dietary material) supporting each parasite.

Fractionation differences between pairings

$\Delta^{15}N$ values of parasite–host pairings varied amongst parasite feeding strategies. Both *Mytilicola orientalis* and stomach nematodes (*Aniskis simplex*) inhabit the digestive tract of their hosts (*Magallana gigas* and *Phocoena phocoena*) and have access to both partially digested food and host tissue. AA-CSIA indicated a strategy of mixed diet feeding as indicated by both parasites residing a half TP above their hosts (0.4 and 0.5, respectively; Fig. 5, 6). *Sacculina carcini*'s feeding strategy is quite different from other parasites in this study as adult *S. carcini* develop extensive rootlet system to directly absorb nutrients from haemolymph associated from a variety of host tissues (Lützen 1984, Bresciani and Høeg 2001, Rowley et al. 2020). This direct tapping into host tissues resulted in a ΔTP_{Bulk} for *S. carcini* of 0.15, indicating minor ^{15}N fractionation during metabolism which was further confirmed by a ΔTP_{5AA} of 0.12 versus locally associated hepatopancreas tissue. Low ΔTP indicates that direct uptake of amino acids from the host is predominantly occurring with limited transamination during metabolism within *S. carcini* which aligns well with the parasite's strategy of inserting roots throughout their host. Low ΔTP indicates that direct uptake of amino acids from the host is predominantly occurring

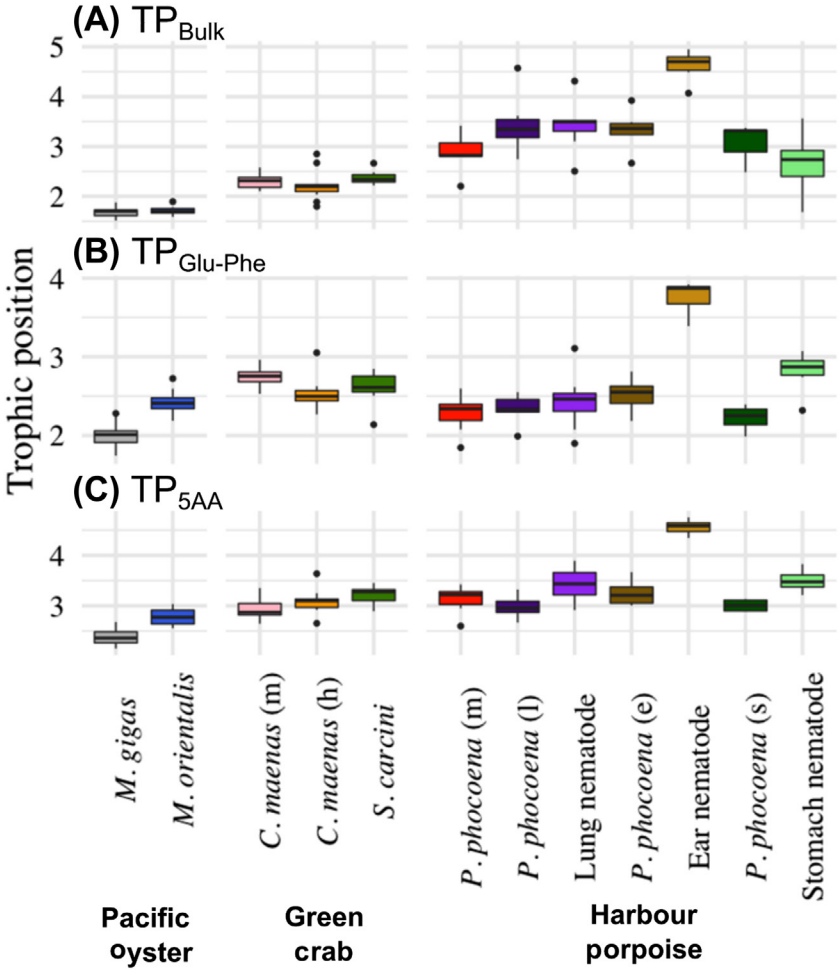

Figure 5. Trophic positions of parasites and hosts. Trophic positions are calculated using (A) bulk $\delta^{15}N$ values (TP_{Bulk}), (B) $\delta^{15}N$ values of Glu and Phe ($TP_{Glu-Phe}$) and (C) $\delta^{15}N$ values of Glu, Val, Ile, Leu and Phe (TP_{5AA}). Median TP values (black line) are presented with boxes and error bars representing the 25th and 10th percentiles, respectively, and dots representing outliers. Host muscle (m) tissue or locally-associated tissues (h = hepatopancreas, l = lung, e = ear canal, s = stomach) were used for comparison of parasite attachment site.

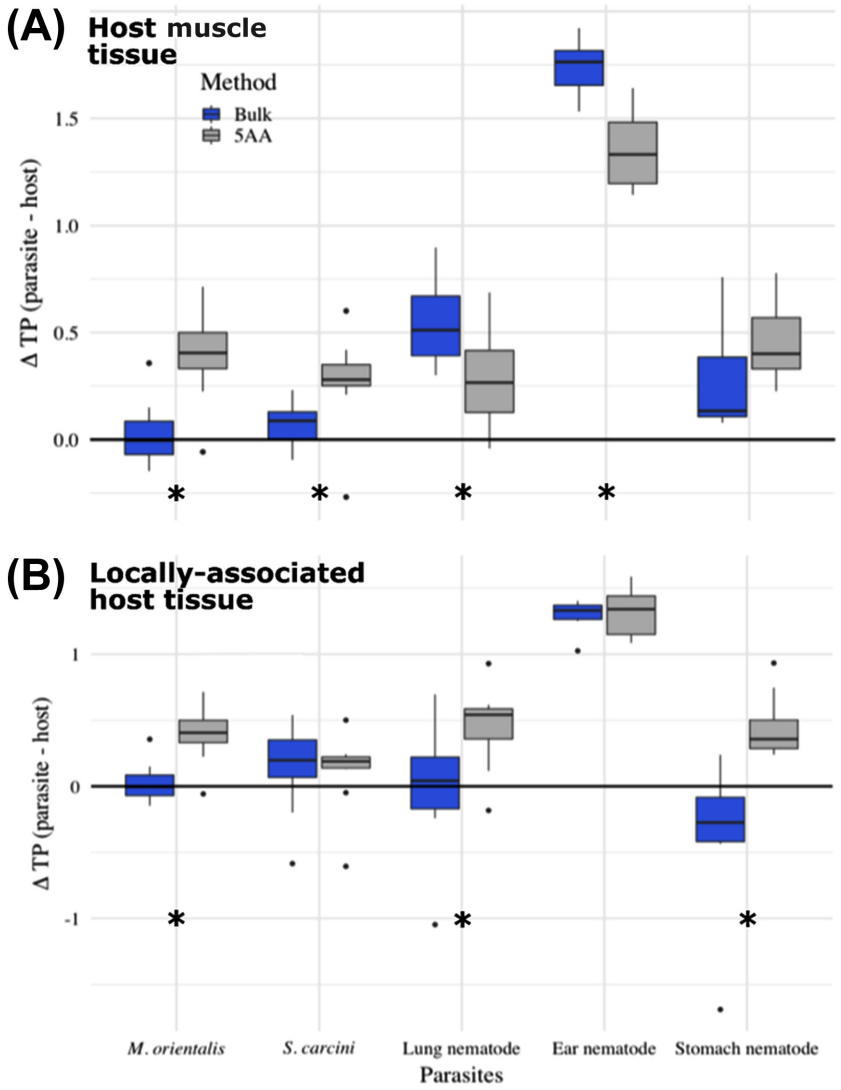

Figure 6. Differences in parasite–host trophic position determined by analysis of bulk nitrogen and amino acid analysis for (A) parasite–host muscle tissue comparison and (B) parasite-locally-associated tissue comparison. Asterisks indicate significant pairwise differences between each amino acid method and the bulk method at an $\alpha = 0.05$.

with limited transamination during metabolism within *S. carcini* which aligns well with the parasite's strategy of inserting roots throughout their host. These results are comparable to cestodes, who also have limited $\Delta^{15}N$ values when compared to their hosts (Boag et al. 1998, Kamiya et al. 2019) due to direct assimilation of compounds using a syncytial, 'microtrich'-covered tegument (Goater et al. 2014) instead of digestion and metabolism of host tissue (Behrmann-Godel and Yohannes 2015). Due to direct uptake of AAs, limited AA transamination occurs prior to incorporation into parasite tissue resulting in a $\Delta^{15}N$ value that is close to zero versus the host's diet.

Parasite feeding strategy differences do not entirely explain $\Delta^{15}N$ differences observed between parasite–host pairings. The lung (*Pseudalius inflexus* and *Torynurus convolutus*) and ear (*Stenurus minor*) nematodes were expected to have similarly high ΔTPs as both have complete digestive tracts (Goater et al. 2014) and feed on their locally-associated tissues of the harbour porpoise. However, the ear nematode had considerably higher ΔTP estimates for both methods (~1.3) than the lung nematode (0.3–0.5; Fig. 5, 6) that is likely not solely a result of feeding style differences. These large variations in $\Delta^{15}N$ values between relatively closely related parasitic species has been observed previously (Riekenberg et al. 2021a). They are not unique to nematodes as Deudero et al. (2002) found that different species of parasitic copepods on the same host exhibited very different $\delta^{15}N$ values. Atypical ^{15}N enrichments in parasites may potentially be explained by metabolic processes unique to each parasite taxon and Kamiya et al. (2019) and Thieltges et al. (2019) indicated $\Delta^{15}N$ variations in parasite–host pairings may be related to parasite phylogenetic histories. However, despite the lung and ear parasites in this study (*P. inflexus*, *T. convolutes* and *S. minor*) all being nematodes of the same family (*Pseudaliidae*),

they maintain markedly different trophic relationships with their hosts. This result implies that utilizing the same parasite–host $\Delta^{15}N$ values to determine TP_{Bulk} for closely related parasites in food webs is unlikely to provide consistently realistic results. The metabolic capabilities of nematodes appear to vary between genus to an extent where bulk-SIA may not provide enough information to reliably resolve trophic interactions between the parasite and host without further characterization of the individual metabolic pathways and TDFs that are appropriate for each genus or species.

The considerable increase in $\Delta^{15}N$ between the ear and lung nematodes may be explained due to relatively poor nutritional content of the ear tissue. Consumer $\Delta^{15}N$ values have been observed to negatively correlate to the nutritional value of its diet (Robbins et al. 2010) with increased tissue C:N ratios resulting in increased TDFs due to the increased metabolic processing required to rework dietary material. The C:N ratio of ear tissue was higher than for lung tissue (4.9 versus 3.4, respectively, Supporting information) and comparatively low concentrations occurred for most AAs in ear versus lung tissue. McMahon et al. (2015) observed a negative correlation between AA imbalance (individual trophic AA mol % in diet minus consumer, for this study individual AA concentration in host tissue minus parasite; Supporting information) and TDFs for trophic AAs. In this study, $\Delta^{15}N$ values between parasites and their host tissues were negatively correlated with AA imbalance for Leu, Lys Ser, Tyr and Val for both lung and ear nematodes (Supporting information). Decreased AA availability within ear tissue is likely requiring the nematodes relying on that tissue to biosynthesise more of the AAs that are not readily available resulting in higher $\Delta^{15}N_{AA}$ and $\Delta^{15}N_{Bulk}$ values as more reworking occurs during metabolism. In turn, the higher availability of AAs within lung tissue results in reduced AA imbalance for the lung nematode that allows for less reworking of amino acids, more direct uptake and smaller associated fractionations between parasite and host tissue AAs that may result in a lower $\Delta^{15}N_{AA}$ (Fig. 6).

Changes in AAs driving fractionation

Differences in $\Delta^{15}N$ values between parasites and hosts are partially driven by underlying changes occurring in individual AAs during metabolism. Examining these changes using principal component analyses revealed fractionations largely grouped along those expected for source, trophic and metabolic AA groupings. Source AAs primarily separated across PC2 in the three pairings with significant separation between parasite and host (e.g. *M. orientalis*, lung and ear nematodes; Fig. 4A, C, D), but variable loadings were apparent between individual source AAs (Met, Lys, Phe). This variability may indicate differences in metabolic capacity of individual parasites to metabolize source AAs or that considerable microbial reworking of source AAs occurs in the host gut content prior to parasite uptake. Given that relatively small positive fractionations are expected for source AAs during metabolism (Chikaraishi et al. 2009), it is surprising that source AAs occasionally have comparable loadings as trophic and metabolic AAs. Trophic AAs largely grouped together and drove separation between parasites and hosts predominately across PC1 due to the large fractionations associated with transamination during AA metabolism. The exception was Tyr, which 'canonically' groups within the source AAs with minimal fractionation occurring during metabolism, but consistently grouped with the trophic AAs in this analysis likely indicating that more processing occurred during metabolism which is why it has been grouped in this analysis as a trophic AA. Increased processing of Tyr indicates that normal (i.e. vertebrate) metabolic processing pathways for Tyr may be limited (Tyagi et al. 2015, International Helminth Genomes Consortium 2019) in a variety of parasites and raises the possibility of alternative processing pathways that may occur or that fractionation may be greatly increased during protein deficiency and these possibilities should be examined further in future work to further characterize this relationship. The metabolic AAs Gly and Ser largely separated in the same direction as the source AAs within the parasite–host pairings, but loadings were variable across both principal components with no clear relationship between the parasite–host pairs. This variability is likely due to differing AA metabolism pathways and physiologies between the parasite species. Thr separated on its own in all of the pairings examined, which is expected due to the uniquely large negative fractionation that occurs during its metabolism (Fuller and Petzke 2017) that appears to be maintained between parasite and host, or becomes considerably more negative in $\delta^{15}N$ (e.g. *M. orientalis*; Fig. 2A).

Host muscle versus locally-associated tissue

Large $\Delta^{15}N$ values have been routinely observed between parasites and host muscle tissues and have led to the so-called 'host-tissue isotope mismatch hypothesis' that describes using host muscle tissue values instead of the locally-associated tissue values that the parasite is feeding upon (Pinnegar et al. 2001, Kamiya et al. 2019, Thieltges et al. 2019). By comparing both host muscle and locally-associated tissue differences in this study for all parasite–host pairings except *M. orientalis* – *M.gigas*, we found that the use of locally-associated tissue decreased the variability in ΔTP and improved agreement between the methods due to reduced fractionations associated with ΔTP_{Bulk} and ΔTP_{5AA} (Fig. 6A, B). The ΔTP_{AA} analyses clearly indicate that *S. carcini* is relying on direct uptake of AAs from their host without considerable metabolic reworking and the other four pairings have an increasing proportion of host tissue as a portion of their diets. Increased agreement between the two methods for the *S. carcini*-crab and ear nematode–porpoise pairings is an effect of the removal of additional fractionation between locally-associated and muscle tissues. For the lung and stomach nematode–porpoise pairings, comparing against locally-associated tissue resulted in positive fractionations that indicate metabolism of N from host tissue instead of no difference or a negative relationship indicated by the bulk method (Fig. 6B). More importantly, there appears to be increased agreement between the trophic positions indicated by ΔTP_{AA} regardless of the host tissue

used in the analysis (Fig. 6). This observation serves to further highlight the utility amino acid analysis that integrates variability from underlying $\delta^{15}N$ baseline (e.g. biogeochemical N sources) used by the host to more accurately characterize parasite–host relationships despite the increased labour and cost associated with the method.

Comparing trophic position between methods

AA-CSIA enables observation of differing AA fractionations between parasite–host pairings (e.g. trophic AAs) that accounts for any variations in the underlying N supporting the parasite (e.g. source AAs). The differences between trophic position estimates described by AA-CSIA and bulk-SIA were most apparent between *M. orientalis*-oyster (0.4 versus 0.03, respectively; Fig. 6) and the stomach nematode (*A. simplex*)–harbour porpoise (0.5 versus −0.4, respectively) for locally-associated tissues. The comparable TPs produced by bulk-SIA for the *M. orientalis*-oyster pairing indicate that the parasite's diet predominately consisted of digestive track contents with minimal feeding on host tissue. However, the TPs produced by AA-CSIA placed *M. orientalis* half a trophic position above *M. gigas* indicating a feeding style of a mixed gut-content/host-tissue feeder. This increase in trophic position aligns well with previous bulk-SIA measurements taken from a *M. orientalis* pairing with an alternate bivalve host that indicated a mixed feeding style between gut content (particulate organic matter and microphytobenthos) and host tissues (*M. orientalis–Mytilus edulis* $\Delta^{15}N_{bulk}$ = 1.22‰; Goedknegt et al. 2018a). For the stomach nematode–harbour porpoise pairing, the ΔTP increased when using AA-CSIA (Fig. 6), likely driven by the strong increases in trophic AA $\delta^{15}N$ values (Fig. 4E), despite decreased AA $\delta^{15}N$ values for both metabolic and source AAs. AA-CSIA gives a clearer depiction of these parasite–host relationships than bulk-SIA due to the removal of underlying N baseline variability within the wild caught hosts using source AA values (Chikaraishi et al. 2009) when estimating TPs. The integration of this underlying variability allows for better resolution of small differences in TP between parasite–host pairs as result of mixed feeding strategies (i.e. not solely relying on host tissue or direct uptake of substrates from the host) while accounting for any variations in the underlying biogeochemical N source values that are supporting the host within the food web. Additionally, AA-CSIA allows for the incorporation of multiple AAs which markedly reduces variability within single AA or bulk-SIA measurements and allows a more accurate TP estimation (McCarthy et al. 2007, Nielsen et al. 2015, McMahon and McCarthy 2016, Sabadel et al. 2019). The two AA-CSIA methods (i.e. Glu and Phe and 5AA) provided considerably different estimates for TP for several relationships (e.g. lung nematode for both tissue types, *S. carcini* for muscle tissue and the stomach nematode for locally associated tissue), but both methods seem to reliably capture the differences between parasite and host. The negative value indicated for *S. carcini* versus host muscle tissue falls within the expected range for direct uptake of host substrates that bypass metabolism in the parasite that is expected with *S. carcini*'s feeding style. However, the Glu-Phe method failed to indicate a difference for the lung nematode paired with locally associated tissue which is unexpected as the lung nematodes are likely to be exclusively feeding on host associated material with no access to outside nutrition due to their feeding style and attachment site. The 5AA method indicates feeding on the host materials that likely involves a mixture of parasite metabolism and direct use of host nutrients (ΔTP of 0.5) while Glu-Phe indicates reliance upon direct uptake only (ΔTP of 0). The strong and consistent groupings of both trophic and source amino acids found in the principal component analyses (Fig. 4) indicate that it is appropriate to combine multiple amino acids, but outcomes are predominately similar between the two methods.

Implications for food web ecology

Parasites are ubiquitous in ecosystems, but few studies have incorporated these species into food webs despite their potential to substantially increase diversity and food web complexity. Recent work has quantified the impact on linkage density and complexity (Dunne et al. 2013, Morton 2020) but largely rely solely on ecological observation and inference to define the parasite–host relationships due to practical limitations of sampling and incomplete characterization of parasite feeding styles. Application of AA-CSIA and establishment of best practices to characterize parasite–host interactions will provide a clearer indication of trophic interaction and allow for a more accurate representation of the trophic effects of these relationships throughout the food web. By clarifying feeding strategies such as predation, kleptoparasitism or mixed strategies, trophic structures that consider parasitism will more accurately reflect reality, especially if infected hosts or parasites are significant prey for higher consumers. Work that further incorporates detailed analysis of parasite metabolism and feeding styles may begin to provide more accurate estimates of energy and nutritional flows throughout marine ecosystems.

This work indicates that the best practice to characterize parasite–host trophic interactions is to examine locally-associated host tissue using AA-CSIA with multiple trophic and source AAs for both parasite and host materials. Use of AA-CSIA provides better clarity on parasite–host $\Delta^{15}N$ values due to source AAs allowing for the integration of baseline variability for both the parasite and host that is impossible to identify with bulk-SIA. Incorporation of multiple trophic and source AAs in the TP estimates reduces the variability that can occur within individual AAs. AA-CSIA gave a clearer indication of differences caused by the metabolism of AAs by the parasite across a broad range of trophic positions found throughout the Wadden Sea food web regardless of the type of host tissue compared against. Accounting for both parasite and host N isotopic baselines reduced uncertainty and variability in parasite–host $\Delta^{15}N_{AA}$ values, allowing for a more accurate analysis of these relationships regardless of host TP. Through this work, we have observed a large variability in

TDFs for parasites that will likely not be adequately characterized through the application of a broad 'universal' TDF for parasites within food webs. Individual TDFs will likely need to be defined for each parasite species being examined, as there remain clear differences in TDFs between species contained in the same phyla (e.g. ear, lung and stomach nematodes). This method is time intensive and costly due to the labour needed to properly derivatize the AAs prior to analysis, but AA-CSIA better characterizes the parasite–host relationships using a relatively small amount of tissue (3–5 mg). Many parasites are small, soft bodied and difficult to cleanly sample (e.g. not easily separated from host tissue), and these limitations need to be considered prior to sample preparation. There is potential to successfully analyze smaller tissue amounts (~1 mg), but issues of host material contamination will increase as parasite sample tissue amounts decrease. Pooling samples to achieve sufficient material for analysis may be a valid option considering the additional information and clarity provided by AA-CSIA analysis on parasite–host relationships.

Acknowledgements – We thank Jort Ossebaar and Ronald von Bommel for technical support and Ewout Adriaans, Joshua Dagoy and Bine Keller for sampling support for this project.
Funding – Funding for analysis was provided as part of Tijs Joling's Masters internship supported by both Coastal Ocean Systems and Marine Microbiology and Biogeochemistry departments at NIOZ. Post-mortem research on harbour porpoises in the Netherlands is commissioned by the Dutch Ministry of Agriculture, Nature and Food Quality, embedded under the statutory research tasks of Wageningen UR, with project reference number WOT-04-009-045.

Author contributions

Philip Riekenberg and **Tijs Joling** contributed equally to this publication and each have the right to claim first author in their CV. **Philip Riekenberg**: Conceptualization (equal); Data curation (equal); Formal analysis (equal); Investigation (equal); Methodology (equal); Supervision (equal); Visualization (equal); Writing – original draft (supporting); Writing – review and editing (lead). **Tijs Joling**: Conceptualization (equal); Data curation (lead); Formal analysis (lead); Investigation (equal); Methodology (equal); Validation (equal); Writing – original draft (lead). **Lonneke L. IJsseldijk**: Conceptualization (supporting); Investigation (supporting); Methodology (supporting); Resources (equal); Writing – review and editing (equal). **Andreas M. Waser**: Methodology (equal); Resources (equal); Writing – review and editing (equal). **Marcel van der Meer**: Conceptualization (equal); Formal analysis (equal); Funding acquisition (equal); Investigation (equal); Methodology (equal); Resources (equal); Supervision (supporting); Writing – review and editing (equal). **David W. Thieltges**: Conceptualization (equal); Formal analysis (equal); Funding acquisition (equal); Methodology (equal); Project administration (equal); Resources (equal); Supervision (equal); Writing – review and editing (equal).

Data availability statement

Data available from 4TU. Research Data: Amino acid data set <http://dx.doi.org/10.4121/14747892> and Bulk isotope data set: <http://dx.doi.org/10.4121/14747862>.

References

Amundsen, P.-A. et al. 2009. Food web topology and parasites in the pelagic zone of a subarctic lake. – J. Anim. Ecol. 78: 563–572.
Behrmann-Godel, J. and Yohannes, E. 2015. Multiple isotope analyses of the pike tapeworm *Triaenophorus nodulosus* reveal peculiarities in consumer–diet discrimination patterns. – J. Helminthol. 89: 238–243.
Boag, B. et al. 1998. Wild rabbit host and some parasites show trophic-level relationships for $\delta^{13}C$ and $\delta^{15}N$: a first report. – Isotopes Environ. Health Stud. 34: 81–85.
Bresciani, J. and Høeg, J. T. 2001. Comparative ultrastructure of the root system in *rhizocephalan* barnacles (Crustacea: Cirripedia: Rhizocephala). – J. Morphol. 249: 9–42.
Brosens, L. et al. 1996. Observations on the helminths of harbour porpoises *Phocoena phocoena* and common guillemots *Uria aalge* from the Belgian and German coasts. – Vet. Rec. J. Brit. Vet. Assoc. 139: 254–257.
Caut, S. et al. 2009. Variation in discrimination factors ($\Delta^{15}N$ and $\Delta^{13}C$): the effect of diet isotopic values and applications for diet reconstruction. – J. Appl. Ecol. 46: 443–453.
Chikaraishi, Y. et al. 2007. Metabolic control of nitrogen isotope composition of amino acids in macroalgae and gastropods: implications for aquatic food web studies. – Mar. Ecol. Prog. Ser. 342: 85–90.
Chikaraishi, Y. et al. 2009. Determination of aquatic food-web structure based on compound-specific nitrogen isotopic composition of amino acids. – Limnol. Oceanogr. Methods 7: 740–750.
DeNiro, M. J. and Epstein, S. 1978. Influence of diet on the distribution of carbon isotopes in animals. – Geochim. Cosmochim. Acta 42: 495–506.
Deudero, S. et al. 2002. Insights into fish host–parasite trophic relationships revealed by stable isotope analysis. – Dis. Aquatic Org. 52: 77–86.
Dobson, A. et al. 2008. Homage to Linnaeus: how many parasites? How many hosts? – Proc. Natl Acad. Sci. USA 105: 11482–11489.
Dubois, S. Y. et al. 2009. Digenean trematodes–marine mollusc relationships: a stable isotope study. – Dis. Aquatic Org. 84: 65–77.
Dunne, J. A. et al. 2013. Parasites affect food web structure primarily through increased diversity and complexity. – PLoS Biol. 11: e1001579.
Faulkner, J. et al. 1998. *Stenurus minor* (Metastrongyloidea: Pseudaliidae) infections of the cranial sinuses of the harbour porpoise, *Phocoena phocoena*. – Can. J. Zool. 76: 1209–1216.
Fry, B. 2006. Stable isotope ecology. – Springer.
Fuller, B. T. and Petzke, K. J. 2017. The dietary protein paradox and threonine ^{15}N-depletion: pyridoxal-5′-phosphate enzyme activity as a mechanism for the $\delta^{15}N$ trophic level effect. – Rapid Commun. Mass Spectrom. 31: 705–718.
Gibson, D. I. et al. 1998. A survey of the helminth parasites of cetaceans stranded on the coast of England and Wales during the period 1990–1994. – J. Zool. 244: 563–574.

Goater, T. M. et al. 2014. Parasitism: the diversity and ecology of animal parasites. – Cambridge Univ. Press.
Goedknegt, M. A. et al. 2018a. Trophic relationship between the invasive parasitic copepod *Mytilicola orientalis* and its native blue mussel *Mytilus edulis* host. – Parasitology 145: 814–821.
Goedknegt, M. A. et al. 2018b. Cryptic invasion of a parasitic copepod: compromised identification when morphologically similar invaders co-occur in invaded ecosystems. – PLoS One 13: e0193354.
Herreras, M. V. et al. 1997. Helminth parasites of the digestive tract of the harbour porpoise *Phocoena phocoena* in Danish waters: a comparative geographical analysis. – Dis. Aquatic Org. 28: 163–167.
Hussey, N. E. et al. 2014. Rescaling the trophic structure of marine food webs. – Ecol. Lett. 17: 239–250.
International Helminth Genomes Consortium 2019. Comparative genomics of the major parasitic worms. – Nat. Genet. 51: 163–174.
Jansen, O. E. et al. 2013. Diet of harbor porpoises along the Dutch coast: a combined stable isotope and stomach contents approach. – Mar. Mammal Sci. 29: E295–E311.
Jung, A. S. et al. 2019. Seasonal variation in the diet of estuarine bivalves. – PLoS One 14: e0217003.
Kamiya, E. et al. 2019. Does atypical ^{15}N and ^{13}C enrichment in parasites result from isotope ratio variation of host tissues they are infected? – Limnology 21: 139–149.
Kristensen, T. et al. 2012. The selective advantage of host feminization: a case study of the green crab *Carcinus maenas* and the parasitic barnacle *Sacculina carcini*. – Mar. Biol. 159: 2015–2023.
Kuris, A. M. et al. 2008. Ecosystem energetic implications of parasite and free-living biomass in three estuaries. – Nature 454: 515.
Lafferty, K. D. and Kuris, A. M. 2002. Trophic strategies, animal diversity and body size. – Trends Ecol. Evol. 17: 507–513.
Lafferty, K. D. et al. 2008. Parasites in food webs: the ultimate missing links. – Ecol. Lett. 11: 533–546.
Lehnert, K. et al. 2005. Macroparasites in stranded and bycaught harbour porpoises from German and Norwegian waters. – Dis. Aquatic Org. 64: 265–269.
Lehnert, K. et al. 2010. Transmission of lungworms of harbour porpoises and harbour seals: molecular tools determine potential vertebrate intermediate hosts. – Int. J. Parasitol. 40: 845–853.
Leopold, M. 2015. Eat and be eaten: porpoise diet studies. – Wageningen Univ., Germany.
Lützen, J. 1984. Growth, reproduction and life span in *Sacculina carcini* Thompson (Cirripedia: Rhizocephala) in the Isefjord, Denmark. – Sarsia 69: 91–105.
Marcogliese, D. J. and Cone, D. K. 1997. Food webs: a plea for parasites. – Trends Ecol. Evol. 12: 320–325.
McCarthy, M. D. et al. 2007. Amino acid nitrogen isotopic fractionation patterns as indicators of heterotrophy in plankton, particulate and dissolved organic matter. – Geochim. Cosmochim. Acta 71: 4727–4744.
McCutchan, J. H. et al. 2003. Variation in trophic shift for stable isotope ratios of carbon, nitrogen and sulfur. – Oikos 102: 378–390.
McMahon, K. W. and McCarthy, M. D. 2016. Embracing variability in amino acid $\delta^{15}N$ fractionation: mechanisms, implications and applications for trophic ecology. – Ecosphere 7: e01511.
McMahon, K. W. et al. 2015. Trophic discrimination of nitrogen stable isotopes in amino acids varies with diet quality in a marine fish. – Limnol. Oceanogr. 60: 1076–1087.
Mente, E. et al. 2010. Amino acid analysis in the shore crab *Carcinus maenas* (Decapoda: Brachyura). – J. Crustacean Biol. 30: 643–650.
Mill, A. C. et al. 2007. Explaining isotope trophic-step fractionation: why herbivorous fish are different. – Funct. Ecol. 21: 1137–1145.
Minagawa, M. and Wada, E. 1984. Stepwise enrichment of ^{15}N along food chains: further evidence and the relation between $\delta^{15}N$ and animal age. – Geochim. Cosmochim. Acta 48: 1135–1140.
Morell, M. et al. 2017. Parasites in the inner ear of harbour porpoise: cases from the North and Baltic Seas. – Dis. Aquatic Org. 127: 57–63.
Nagasawa, K. 1990. The life cycle of *Anisakis simplex*: a review. – In: Intestinal anisakiasis in Japan. Springer, pp. 31–40.
Nielsen, J. M. et al. 2015. Meta-analysis of amino acid stable nitrogen isotope ratios for estimating trophic position in marine organisms. – Oecologia 178: 631–642.
O'Connell, T. C. 2017. 'Trophic' and 'source' amino acids in trophic estimation: a likely metabolic explanation. – Oecologia 184: 317–326.
O'Grady, S. P. and Dearing, M. D. 2006. Isotopic insight into host–endosymbiont relationships in Liolaemid lizards. – Oecologia 150: 355–361.
Pinnegar, J. K. et al. 2001. Unusual stable isotope fractionation patterns observed for fish host–parasite trophic relationships. – J. Fish Biol. 59: 494–503.
Popp, B. N. et al. 2007. Insight into the tophic ecology of yellowfin tuna, *Thunnus albacares*, from compound-specific nitrogen isotope analysis of proteinaceous amino acids. – In: Terrestrial ecology. Elsevier, pp. 173–190.
Post, D. M. 2002. Using stable isotopes to estimate trophic position: models, methods and assumptions. – Ecology 83: 703–718.
Powell, A. and Rowley, A. F. 2008. Tissue changes in the shore crab *Carcinus maenas* as a result of infection by the parasitic barnacle *Sacculina carcini*. – Dis. Aquatic Org. 80: 75–79.
Power, M. and Klein, G. M. 2004. Fish host–cestode parasite stable isotope enrichment patterns in marine, estuarine and freshwater fishes from northern Canada. – Isotopes Environ. Health Stud. 40: 257–266.
Pravettoni, V. et al. 2012. *Anisakis simplex*: current knowledge. – Eur. Ann. Allergy Clin. Immunol. 44: 150.
Preston, D. L. et al. 2013. Biomass and productivity of trematode parasites in pond ecosystems. – J. Anim. Ecol. 82: 509–517.
Riekenberg, P. M. et al. 2021a. Impacts of host phylogeny, feeding styles and parasite attachment site on isotopic discrimination in helminths infecting coral reef fish hosts. – Sci. Rep. 11: 1–10.
Riekenberg, P. M. et al. 2021b. Practical considerations for improved reliability and precision during determination of $\delta^{15}N$ values in amino acids using a single combined oxidation–reduction reactor. – Rapid Commun. Mass Spectrom. 34: e8797.
Robbins, C. T. et al. 2010. The impact of protein quality on stable nitrogen isotope ratio discrimination and assimilated diet estimation. – Oecologia 162: 571–579.
Rowley, A. F. et al. 2020. Prevalence and histopathology of the parasitic barnacle, *Sacculina carcini* in shore crabs, *Carcinus maenas*. – J. Invertebr. Pathol. 171: 107338.
Sabadel, A. J. M. et al. 2016. Compound-specific isotope analysis of amino acids: a tool to unravel complex symbiotic trophic relationships. – Food Webs 6: 9–18.
Sabadel, A. J. M. et al. 2019. Stable-isotope analysis: a neglected tool for placing parasites in food webs. – J. Helminthol. 93: 1–7.
Sánchez Barranco, V. et al. 2020. Trophic position, elemental ratios and nitrogen transfer in a planktonic host–parasite–consumer food chain including a fungal parasite. – Oecologia 194: 541–554.

Stock, J. H. 1993. Copepoda (Crustacea) associated with commercial and non-commercial Bivalvia in the East Scheldt, the Netherlands. – Bijdragen Dierkunde 63: 61–64.
ten Doeschate, M. T. I. et al. 2017. Quantifying parasite presence in relation to biological parameters of harbour porpoises *Phocoena phocoena* stranded on the Dutch coast. – Dis. Aquatic Org. 127: 49–56.
Thieltges, D. W. et al. 2013. Parasites in the Wadden Sea food web. – J. Sea Res. 82: 122–133.
Thieltges, D. W. et al. 2019. Parasites and stable isotopes: a comparative analysis of isotopic discrimination in parasitic trophic interactions. – Oikos 128: 1329–1339.
Troost, K. 2010. Causes and effects of a highly successful marine invasion: case-study of the introduced Pacific oyster *Crassostrea gigas* in continental NW European estuaries. – J. Sea Res. 64: 145–165.
Tyagi, R. et al. 2015. Pan-phylum comparison of nematode metabolic potential. – PLoS Negl. Trop. Dis. 9: e0003788.
Waser, A. M. et al. 2016. Tidal elevation and parasitism: patterns of infection by the rhizocephalan parasite *Sacculina carcini* in shore crabs *Carcinus maenas*. – Mar. Ecol. Prog. Ser. 545: 215–225.
Whiteman, J. P. et al. 2019. A guide to using compound-specific stable isotope analysis to study the fates of molecules in organisms and ecosystems. – Diversity 11: 8.
Yarnes, C. T. and Herszage, J. 2017. The relative influence of derivatization and normalization procedures on the compound-specific stable isotope analysis of nitrogen in amino acids. – Rapid Commun. Mass Spectrom. 31: 693–704.
Zetlmeisl, C. et al. 2011. Parasites of the shore crab *Carcinus maenas* (L.): implications for reproductive potential and invasion success. – Parasitology 138: 394–401.